Structure of superdeformed bands in ^{195}Hg

G. Hackman,[1] R. Krücken,[2] R. V. F. Janssens,[1] M. A. Deleplanque,[2] M. P. Carpenter,[1] D. Ackermann,[1] I. Ahmad,[1] H. Amro,[1] S. Asztalos,[2] D. J. Blumenthal,[1] R. M. Clark,[2] R. M. Diamond,[2] P. Fallon,[2] S. M. Fischer,[1] B. Herskind,[3] T. L. Khoo,[1] T. Lauritsen,[1] I-Y. Lee,[2] R. W. MacLeod,[2] A. O. Macchiavelli,[2] D. Nisius,[1] G. J. Schmid,[2] F. S. Stephens,[2] K. Vetter,[2] and R. Wyss[4]

[1]*Argonne National Laboratory, Argonne, Illinois 60439*

[2]*E.O. Lawrence Berkeley National Laboratory, Berkeley, California 94720*

[3]*Niels Bohr Institute, University of Copenhagen, Copenhagen, Denmark*

[4]*Manne Siegbahn Institute, S-104 05 Stockholm, Sweden*

(Received 29 August 1996)

Four new superdeformed bands have been observed with the Gammasphere array and have been assigned to the ^{195}Hg nucleus. Two of the bands are interpreted as signature partners most likely based on $N_{\rm osc}=6$ neutron quasiparticles coupled to a superdeformed core, while the other two appear to be based on a $j_{15/2}$ intruder orbital. These four bands do not exhibit a simple, ''identical bands'' relationship to other superdeformed bands in this mass region. [S0556-2813(97)06001-9]

PACS number(s): 27.80.+w, 23.20.Lv, 21.10.Re, 21.60.Ev

I. INTRODUCTION

Superdeformed (SD) bands of nuclei with mass number $A\sim 190$ provide an excellent opportunity to explore nuclear structure phenomena at large deformation in the presence of pairing. Mean-field calculations predict stable minima in the total energy surface of many nuclei in this region at large deformation [1–3]. This is due to the presence of large shell gaps at neutron number $N=112$ and proton numbers $Z=80$ and $Z=82$ for values of the quadrupole deformation parameter $\beta_2\sim 0.5$. These predictions have been borne out by experiments: Following the discovery of a SD band in the nucleus ^{191}Hg [4], similar structures have been reported in the $^{189-194}$Hg isotopes, in $^{192-198}$Pb, in ^{198}Po, and in the odd-proton nuclei $^{191-195}$Tl, $^{195-197}$Bi, and ^{191}Au [5]. At low rotational frequencies ($\hbar\omega<0.3$ MeV), the dynamic moments of inertia ($\mathcal{J}^{(2)}$) of many of these SD bands can be satisfactorily described when pairing is included as a first-order perturbation to the mean field [6]. Recently, the inclusion of higher-order pairing terms [7] treated self-consistently by the Lipkin-Nogami method [8] has been shown to improve the ability of cranked shell-model calculations to reproduce the behavior of SD bands up to the highest rotational frequencies observed. Similar success was also found in Hartree-Fock-Bogolyubov calculations with a density-dependent surface-delta interaction [9] or with a Gogny force [10]. While the successes of these models have been impressive, some open questions remain. For example, the existence of ''identical'' bands, i.e., bands with essentially the same γ-ray energies in neighboring nuclei, has not been explained satisfactorily thus far.

The various calculations mentioned above also predict that a second, large SD neutron shell gap should occur at $N=116$. Thus, $^{196}_{80}\mathrm{Hg}_{116}$ could be considered as a doubly magic SD nucleus. Numerous attempts to investigate superdeformation in this nucleus using light projectiles such as ^{18}O or ^{9}Be [11,12] have proved unsuccessful because ^{196}Hg cannot be easily populated at an appropriate excitation energy and angular momentum. Indeed, there are no suitable projectile-target combinations for the most commonly used heavy-ion-induced fusion-evaporation reactions [i.e., for the usual (HI, $4n$ or $5n$) reaction channels].

Here, we report on the first observation of superdeformation in ^{195}Hg, a nucleus which can be regarded as a neutron hole with respect to a ^{196}Hg core. Four SD bands have been observed following a $3n$ fusion-evaporation reaction. The bands can be satisfactorily understood in the framework of cranked shell-model calculations. However, none of them is found to exhibit an ''identical band'' relationship with other SD bands of the region.

The experiment and data reduction will be discussed in Sec. II. The new bands are presented in Sec. III along with possible spin assignments. In Sec. IV, the bands are interpreted within the framework of the cranking model by comparisons to SD bands in other odd Hg isotopes and to mean-field calculations. Configurations are proposed, and the role of a possible ^{196}Hg core is discussed. Section V summarizes the results.

II. EXPERIMENT AND DATA REDUCTION

The reaction ^{150}Nd(^{48}Ca,xn) was employed to populate high-spin states in the nuclei $^{198-x}$Hg. The beam, with a nominal energy of 201 MeV, was provided by the 88-inch cyclotron at the Lawrence Berkeley National Laboratory. A stack of two targets was used, each consisting of a ~ 500 μg/cm^2 isotopically enriched ^{150}Nd foil, with ~ 200 μg/cm^2 of Au evaporated on one side and ~ 400 μg/cm^2 on the other to prevent oxidation of the Nd. The targets were stacked with the beam impinging upon the thicker Au layers. The reaction was selected for optimal population of ^{194}Hg SD bands, and the results from the study of this nucleus are published elsewhere [13]. Gamma rays following fusion-evaporation reactions were detected with the Gammasphere array [14], which for this experiment comprised 72 Compton-suppressed high-purity germanium (HPGe) spectrometers. Events satisfying a minimum coincidence require-

ment that four suppressed spectrometers fire in prompt coincidence were written on magnetic tape. The digitized energy signals were gain matched on line to a nominal dispersion of 0.125 keV/channel based on gain and offset coefficients determined prior to the experiment with a calibration source. The data written on tape were subsequently filtered off line and checked for prompt coincidence timing. At the same time, fine gain and Doppler corrections ($v/c=2.02\%$) were applied. A total of 6.1×10^8 triple-, 3.4×10^8 quadruple-, and 0.9×10^8 higher-fold events were available for subsequent analysis.

The search for new SD bands in the data was performed with the quadruple-coincidence version of the ANDBAND automatic SD search algorithm, which is described in detail in Ref. [15]. The input parameters specified cascades of a minimum of ten transitions with starting energies, γ-ray energy spacings, and changes in the $\mathcal{J}^{(2)}$ moments typical of the Hg, Tl, and Pb SD bands. Approximately 10^4 trial bands were tested. Each candidate band from the list reported by ANDBAND was subsequently inspected by generating the spectrum corresponding to all possible combinations of double gates placed on a γ-γ-γ coincidence cube. This was done with the XMLEV implementation of the LEVIT8R code [16]. The advantage of this graphical analysis is that the known level structure of nuclei present in the data set can be included in a level scheme input file. This is important for identifying contributions to the coincidence spectra from strong coincidences not directly related to the trial band in question, such as yrast and other non-SD cascades or known SD bands with similar transition energies.

III. RESULTS

From these analyses four cascades consistent with SD decay, hereafter labeled bands (a), (b), (c), and (d), were identified, none of which had been reported previously. To assign these new cascades to a specific residual nucleus, the individual spectra corresponding to each γ_1-γ_2 coincidence gate were first inspected for peaks larger than those in the new band. Such spectra most likely contain contaminants and could provide misleading evidence for coincidence relationships following the decay of the SD states to lower-lying yrast and near-yrast states. Of the $\sim$100 unique double-gate combinations for bands (a), (c), and (d), only about one-quarter could be used, while for band (b), approximately one-half of the double gates were acceptable. Based on the final spectra resulting from the sum of all clean gates, the new bands (a), (b), and (c) were found *not* to be in coincidence with low-spin transitions of either ^{194}Hg or ^{193}Hg. Charged particle evaporation channels were not observed, and the only remaining possibility was ^{195}Hg. The case of band (d) was more complicated because many of the gates below 650 keV were in close proximity to known transitions of SD bands 1 and 3 of ^{194}Hg. However, in a careful analysis of the coincidence data it was possible to disentangle the contributions from deexcitation within the two Hg isotopes. For example, yields of yrast transitions following the deexcitation of the two ^{194}Hg SD bands could be fully accounted for. Furthermore, in the difference spectrum between the observed data and the calculated yields for band (d), these ^{194}Hg yrast lines were not present.

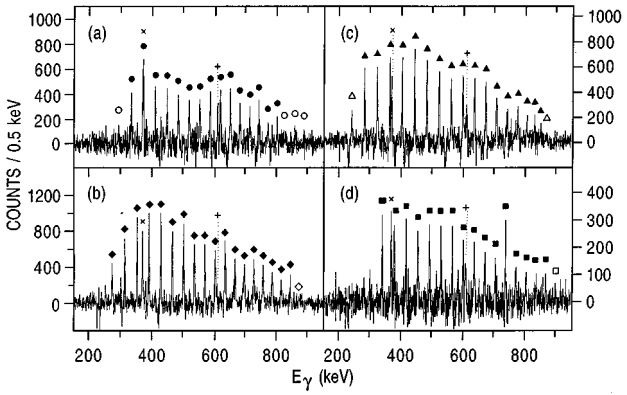

FIG. 1. Sum of clean triple-gated spectra of the new bands in ^{195}Hg, i.e., (a), (b), (c), and (d). In-band γ rays are indicated by solid symbols, open for tentative transitions. The 371 and 611 keV yrast lines on which the assignment is based are marked by $\times$ and $+$, respectively.

The assignments were confirmed by studying the quadruple-γ coincidence data. For each band, the list of clean double gates was used to construct clean triple gates. Figure 1 shows the sums of these coincidence spectra, background corrected by the ''Φ operator'' global background subtraction method described in Ref. [17]. The most compelling evidence supporting an assignment to the ^{195}Hg nucleus is a readily identifiable 371 keV line found to be in coincidence with bands (b), (c), and (d). This γ ray corresponds to the $17/2^+\rightarrow13/2^+$ transition of the $i_{13/2}$ yrast band of ^{195}Hg [18]. The 371 keV line is partially obscured in band (a) by a SD transition. There is also evidence in all four spectra for the 611 keV transition, which belongs to the ^{195}Hg yrast cascade ($21/2^+\rightarrow17/2^+$). Transitions within 1 keV of this line are also assigned to ^{193}Hg ($21/2^-\rightarrow21/2^+$) and ^{194}Hg ($12^-\rightarrow10^-$); however, in our data neither is observed in strong coincidence with the known ^{193,194}Hg SD bands. The spectrum of band (d) includes only those triple-gate combinations with at least one gate above 650 keV to reduce any contribution to the spectrum from the ^{194}Hg bands. The assignment of these bands to ^{195}Hg was confirmed in the analysis of a gated xmlev cube, where for any event with one γ ray satisfying a 371 keV gate, the remaining γ rays in the event were histogrammed. The yields for all four bands remained constant relative to other ^{195}Hg lines, while the contaminant SD bands of ^{194,193}Hg were strongly attenuated.

Table I presents the transition energies and intensities of the four SD bands. This information was determined by performing fits to the coincidence cube with XMLEV. The energies of transitions in band (a) are nearly equal to the average of consecutive transitions of band (b), and vice versa. This is the pattern expected for $E2$ transitions of strongly coupled signature partner bands. For some transitions in Table I, obtaining accurate values for the energies and intensities was complicated because of their close proximity in the coincidence cube to strong yrast or near-yrast transitions. Similarly, it was not possible to extract angular distributions for band (a), (c), or (d). For band (b), the statistics were only sufficient to say that, for clean transitions, the angular distributions had A_2 coefficients with positive values, as one

TABLE I. Energies and intensities (normalized to 100% in the plateau region in each band) of gamma-ray transitions assigned to the four ^{195}Hg SD bands. Tentative transitions are given in brackets.

Band (a)		Band (b)		Band (c)		Band (d)	
E_γ (keV)	$I_\gamma^{\rm rel}$ (%)	E_γ (keV)	$I_\gamma^{\rm rel}$ (%)	E_γ (keV)	$I_\gamma^{\rm rel}$ (%)	E_γ (keV)	$I_\gamma^{\rm rel}$ (%)
				[244]			
[294]		273.9(2)	49(5)	284.5(1)	76(5)		
333.9(1)	64(7)	314.2(1)	64(5)	325.0(1)	92(6)	341.9(1)	89(16)
372.8(3)	107(30)	353.5(1)	88(5)	365.4(1)	99(6)	380.9(1)	106(22)
411.2(3)	65(8)	392.2(1)	92(5)	405.3(1)	93(6)	419.1(1)	81(16)
448.4(1)	86(7)	429.9(1)	100(6)	445.0(1)	97(6)	457.2(1)	100(16)
484.7(1)	96(9)	466.9(1)	94(5)	484.5(1)	99(6)	494.5(1)	103(16)
519.8(1)	92(10)	502.8(1)	102(5)	523.6(1)	103(6)	531.4(1)	90(17)
554.0(1)	101(9)	537.6(1)	105(6)	562.1(1)	82(7)	567.6(1)	97(18)
587.5(2)	100(9)	571.3(1)	87(6)	600.0(1)	101(7)	602.8(1)	100(18)
620.3(3)	106(10)	604.2(1)	104(7)	637.1(4)	100(9)	638.1(1)	102(21)
652.2(3)	105(9)	636.2(4)	116(8)	673.4(2)	107(7)	672.4(2)	112(22)
683.2(2)	70(7)	668.1(1)	108(7)	708.7(4)	112(9)	705.9(2)	100(26)
714.2(3)	62(8)	698.1(2)	96(7)	742.2(9)	64(10)	739.1(8)	75(20)
743.2(8)	41(7)	728.3(2)	69(5)	776.1(3)	54(4)	771.6(2)	64(18)
772.8(4)	34(4)	757.8(2)	71(5)	805.0(4)	33(5)	803.4(5)	40(16)
802.2(9)	32(4)	787.2(3)	54(5)	829.1(6)	22(4)	836.1(5)	38(15)
[832]		815.8(9)	38(4)	848.5(5)	17(4)	868.0(6)	38(17)
[861]		845.0(9)	16(3)	[868]		[899]	
[887]		[874]					

would expect for stretched $E2$ transitions. The total flux through each of the four SD bands was determined to be 0.4(2)%, 0.9(3)%, 0.4(1)%, and 0.6(3)% of the intensity of the 371 keV transition. Since the compound nuclei recoil out of the focus of the HPGe detectors, the presence of any yrast or near-yrast isomer with a half-life $\geqslant 5$ ns in ^{195}Hg could possibly result in a reduced yield for some yrast transitions. Hence, the SD yields reported above should perhaps be regarded as upper limits.

IV. DISCUSSION

The data of Table I have been used to derive the $\mathcal{J}^{(2)}$ moments of inertia which are presented as a function of the rotational frequency $\hbar\omega$ in Fig. 2. (See Ref. [19] for the definition of these quantities.) Tentative transitions (given in brackets in Table I) are not included in the discussion. Three important observations are immediately obvious from this figure. First, the $\mathcal{J}^{(2)}$ values for bands (a) and (b) experience a smooth rise over the entire frequency range, a behavior which is the same as that seen in ^{194}Hg and in most other SD bands of the $A\sim 190$ region. Second, band (c) displays a markedly different behavior as the $\mathcal{J}^{(2)}$ moment is almost constant at frequencies $\hbar\omega < 0.4$ MeV with a sharp rise beyond that. Third, the $\mathcal{J}^{(2)}$ moment of band (d) lies between that of bands (a), (b), and (c), but does not experience the sharp upturn at 0.4 MeV: In fact, it may have reached a constant value or have begun to turn down at this frequency. Finally, at the lowest frequencies, the $\mathcal{J}^{(2)}$ values for all four ^{195}Hg bands are larger than that of band 1 in ^{194}Hg.

In an attempt to understand the quasiparticle configurations associated with these bands, the data can be presented in terms of the experimental Routhians (e') and aligned spins (i_x) [19], which are shown in Fig. 3. The computation of these quantities depends on the spins and, for e', excitation energies of the bands, as well as on a phenomenological representation of the energy associated with the rotating core. The intensities of the four bands are too small to obtain guidance on the spins and excitation energies of the SD states from the decay into the normal-deformed, yrast, and near-yrast states. Thus, the spins have been estimated with a fit of the Harris expansion to the measured $\mathcal{J}^{(2)}$ values as a function of frequency [20]. In this way, the 334 keV γ ray of

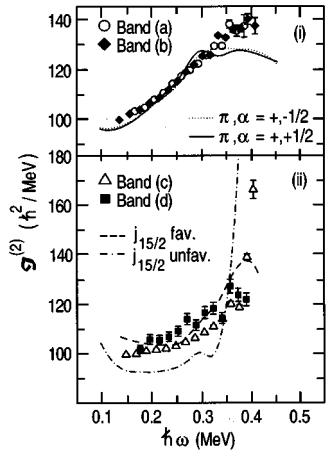

FIG. 2. Experimental (data points) and calculated (curves) dynamic moments of inertia $\mathcal{J}^{(2)}$ as a function of rotational frequency $\hbar\omega$. Panel (i): bands (a) and (b) compared to calculations for the $(\pi,\alpha)=(+,\pm 1/2)$ (ν [624]9/2) configurations. Panel (ii): bands (c) and (d) and calculations for $\nu j_{15/2}$ favored and unfavored configurations.

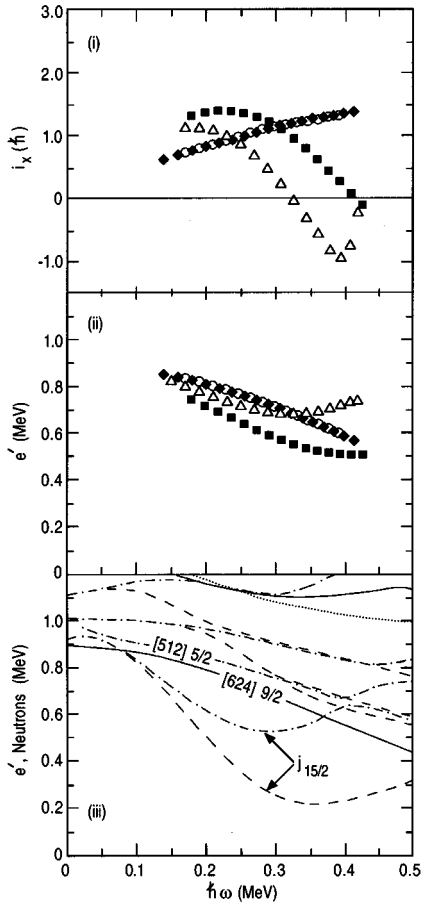

FIG. 3. Panels (i) and (ii): experimental aligned spin i_x and Routhians e' for the ^{195}Hg SD bands. Spins and excitation energies assumed for the bands are described in the text. The reference was derived from ^{194}Hg. In both plots the data for band (a) are shown with open circles; band (b), solid diamonds; band (c), open up triangles; band (d), solid squares. Panel (iii): quasineutron Routhians calculated with the Woods-Saxon mean field and Lipkin-Nogami pairing described in the text. The intruder orbitals relevant to the discussion are labeled as $j_{15/2}$ while the other orbitals of interest are identified with their asymptotic Nilsson numbers.

band (a) is assigned as a $33/2\rightarrow 29/2$ transition, while the 274 keV line of band (b) is assigned as $27/2\rightarrow 23/2$. This is consistent with these two bands being signature partners. The final-state spins of the lowest firmly assigned γ-ray transitions in bands (c) and (d) have been assigned as 25/2 and 31/2, respectively, even though spins higher by $1\hbar$ cannot be ruled out from the results of the fit. The proposed spin sequence is favored because of the configuration assignment discussed below.[1] The excitation energies have been selected such that e' would extrapolate at $\hbar\omega=0$ to 0.9 MeV for bands (a) and (b) and 1.0 MeV for bands (c) and (d). These values have been selected to match the [624]9/2 and $j_{15/2}$ quasineutron energies at $\hbar\omega=0$ [see Fig. 3(iii) and discussion below]. For bands (a) and (b), the excitation energies are further constrained such that the difference is consistent with the assumption that they are strongly coupled signature partners. Finally, band 1 of ^{194}Hg was taken as the reference.[2] It is clear that the Routhians for bands (a) and (b) indicate that these bands do not exhibit any signature splitting and, thus, remain strongly coupled over the entire frequency range. The two bands also *appear* to gain about one unit in alignment with respect to the (^{194}Hg) reference. The Routhians and alignments for bands (c) and (d) are quite different as can be seen from both the curvature of the Routhian at $\hbar\omega>0.3$ MeV and the rapid loss of alignment over the entire frequency range.

The observations derived from the inspection of Figs. 2 and 3 provide clues about possible configuration assignments for the four SD bands. The absence of signature splitting over the entire frequency range for bands (a) and (b) suggests that the associated configuration corresponds to a strongly coupled neutron orbital whose wave function remains relatively pure, even at the highest frequencies. The Routhian which originates from the positive-parity [624]9/2 orbital at $\hbar\omega=0$ is a good candidate since, as seen in Fig. 3(iii), it is one of the few orbitals of this parity expected to be near the Fermi surface. One would expect a band based on this odd neutron to exhibit the same behavior as nearby even-even nuclei; specifically, it should exhibit the same rise in $\mathcal{J}^{(2)}$ as seen in ^{194}Hg. This rise has been ascribed to the gradual alignment of a $j_{15/2}$ quasineutron pair at low frequency ($\hbar\omega\sim 0.2$ MeV) followed by the the alignment of an $i_{13/2}$ quasiproton pair ($\hbar\omega\sim 0.35$ MeV). The behaviors of the $\mathcal{J}^{(2)}$ moments of bands (c) and (d) are reminiscent of that seen in certain SD bands of the lighter odd-N isotopes ^{191,193}Hg which have been associated with a $j_{15/2}$ neutron intruder configuration [21,22]. In these cases, the constant value of the $\mathcal{J}^{(2)}$ moment at low frequencies can be understood as resulting from the blocking of the $j_{15/2}$ neutron alignment. This also accounts for the sharp drop in alignment in Fig. 3, since i_x is calculated with respect to a ^{194}Hg reference where the $j_{15/2}$ neutron pair alignment is not blocked. A proton pair alignment at high frequencies contributes to the increase in $\mathcal{J}^{(2)}$ of these bands above $\hbar\omega=0.3$ MeV. Since the unfavored signature of the $j_{15/2}$ bands in both ^{191}Hg and ^{193}Hg has a lower $\mathcal{J}^{(2)}$ value at low frequency than the favored signature, it is proposed that, by analogy, band (c) of ^{195}Hg is the unfavored $j_{15/2}$ band and band (d) the favored partner.

In order to place these considerations on a stronger footing, cranked shell-model (CSM) calculations have been performed. In the latter, a revised parametrization of the Woods-Saxon potential was used [23] which yields moments of inertia which no longer require a renormalization [24], and quadrupole pairing was added to the standard monopole term [7]. Both pairing and deformation were varied self-consistently by means of the Lipkin-Nogami method [8]. The results of the calculations are presented in Fig. 2.

Calculations are given for the two signatures of the $j_{15/2}$ orbital as well as for the excitations based on the [624]9/2 orbital which lies in the vicinity of the Fermi surface at the

[1]It should, however, also be noted that the spin fitting procedure is less reliable for bands with significant alignment, such as high-j intruder bands.

[2]Arguably, the ^{192}Hg core could have been used instead; this detail would change neither the substance of our discussion nor our conclusions.

large deformations ($\beta_2 \sim 0.48$, $\beta_4 \sim 0.06$). The calculated behavior of the $\mathcal{J}^{(2)}$ moments for the [624]9/2 configuration adequately reproduces the experimental data for bands (a) and (b). In particular, the [624]9/2 configuration exhibits a rise of $\mathcal{J}^{(2)}$ with frequency, which is similar in magnitude to that found in the data. Furthermore, the signature splitting in the calculations is very small, as is observed for bands (a) and (b). However, the flattening and downturn of the $\mathcal{J}^{(2)}$ curves which is predicted to occur at the frequencies $\hbar\omega > 0.32$ MeV seem absent from the data. A similar discrepancy was observed in ^{194}Hg [25]; i.e., the downturn in the experimental $\mathcal{J}^{(2)}$ occurs at a slightly higher frequency than in the calculations, where it follows the completion of the $j_{15/2}$ neutron alignment at $\hbar\omega \sim 0.32$ MeV and of the $i_{13/2}$ proton alignment at $\hbar\omega \sim 0.4$ MeV. This discrepancy remains a (minor) deficiency of the calculations.

In the same way, the calculations for the $j_{15/2}$ orbital reproduce the overall behavior of bands (c) and (d). The unfavored $\nu j_{15/2}$ configuration is crossed at $\hbar\omega \simeq 0.35$ MeV by the one-quasiparticle [512]5/2 excitation, which results in the rather sharp increase in the calculated $\mathcal{J}^{(2)}$ at $\hbar\omega \sim 0.35$ MeV. (In Fig. 2, the curve has not been followed beyond that point.) This crossing also occurs in the calculations for the favored signature, but at the very low frequency of $\hbar\omega \sim 0.1$ MeV, a point that is not observed in the present data for band (d). The exact frequency of this crossing is sensitive to the energy of the neutron $j_{15/2}$ subshell; in particular, the fact that the calculated crossing comes at a lower frequency than what is observed experimentally in band (c) may imply that the $j_{15/2}$ shell is too high in excitation energy relative to the $f_{7/2}$ shell in the calculations, as has been noted elsewhere [22].

One of the startling and as yet not satisfactorily explained properties of SD bands is the so-called ''identical bands'' phenomenon. This refers to the observation that bands in nuclei differing by several mass units can have transitions of the same energy (within 1–2 keV). The concept has also been used in a less restrictive way to describe bands which exhibit identical $\mathcal{J}^{(2)}$ moments of inertia [26]. As a large number of bands in the Hg isotopes can be characterized by such relations [27], it seemed worthwhile to investigate if this was also the case for the four new bands observed here. The four bands were compared to the known SD bands in the Hg or Pb isotopes, but no significant relationship to any of them was found. This point is illustrated, to a degree, in Fig. 4. The $\mathcal{J}^{(2)}$ moments for ^{195}Hg bands (a) and (b) are $\sim 5\%$ larger than those observed for band 1 of ^{194,192}Hg. The lack of a simple ''identicality'' relationship is also evident in Fig. 3, where the aligned spin i_x represents an attempt to relate the four bands to band 1 of ^{194}Hg. It is clear from the figure that none of the bands results in a constant i_x value. Similarly, computations of incremental alignments as defined in Ref. [27], using ^{192}Hg or ^{194}Hg as a reference, result in curves which vary with frequency without reaching any of the ''quantized'' values of ± 0.5, 0, or 1.

One possible explanation for the nonobservation of quantized incremental alignments is that the four SD bands in ^{195}Hg are best described as neutron-hole configurations associated with a ^{196}Hg core, in the same way that the four SD bands of ^{191}Hg are related to ^{192}Hg [21]. If this were the case, an identical bands relationship with the ^{196}Hg yrast SD band would be predicted, at least for bands (a) and (b) of ^{195}Hg. The situation for bands (c) and (d) would be different because of the blocking of the $\nu j_{15/2}$ alignment discussed above. For this scenario to be true, the properties of the ^{196}Hg core would have to be different from those of the ^{194}Hg or ^{192}Hg cores. To explore this possibility further, the dynamic moments of inertia were calculated for the yrast SD configurations of even mercury isotopes ^{192,194,196}Hg. These calculations treat both pairing and deformation self-consistently, and the only independent variable contributing to the differences in $\mathcal{J}^{(2)}$ moments for the three isotopes shown in Fig. 4 is the location of the Fermi surface. The $\mathcal{J}^{(2)}$ moment of ^{196}Hg is indeed higher than that of ^{194}Hg at frequencies $\hbar\omega > 0.2$ MeV. This is a necessary *but not sufficient* condition for ^{195}Hg bands to share identical bands relationships with ^{196}Hg. Microscopically, the change in the Fermi level results in a stronger proton alignment as well as in a neutron alignment occurring over a larger frequency range in ^{196}Hg than in ^{194}Hg.

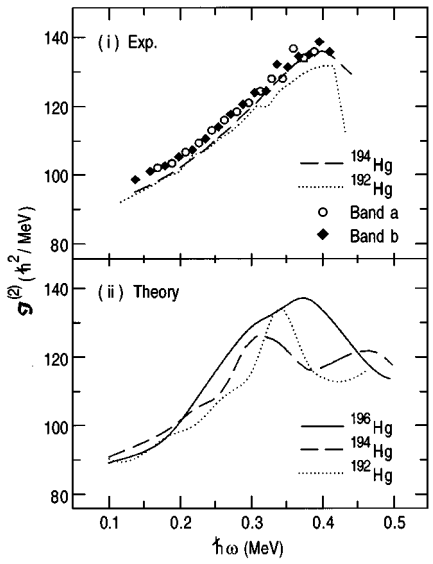

FIG. 4. Panel (i): $\mathcal{J}^{(2)}$ moments of inertia for ^{195}Hg bands (a),(b), symbols; ^{194}Hg band 1, solid line; ^{192}Hg band 1, dashed line. Panel (ii): calculated $\mathcal{J}^{(2)}$ moments of inertia for the even-even ^{192,194,196}Hg nuclei.

At this point it is important to note that the previous discussion requires the additional assumption that the mechanism which yields identical bands is independent of neutron number. However, calculations of the interaction strength between neutron high-j orbitals indicate a maximum for $^{192-194}$Hg, as discussed in detail in Ref. [28]. It is conceivable that for $A = 192 \rightarrow 194$, the relatively constant interaction strength in the vicinity of this maximum results in a core which remains unaffected by a change of the Fermi level. Farther from this local maximum, the core may be less robust to addition (or removal) of neutrons as the interaction strength changes more rapidly. If this scenario is correct, one would predict that the ^{196}Hg SD band *should not* exhibit an identical bands relationship to ^{195}Hg bands (a) and (b). Thus, one is left with two conflicting predictions, and the resolution of the issue will come only from the experimental discovery of the ^{196}Hg SD band, a measurement which is cer-

TABLE II. Summary of SD bands in ^{195}Hg: population intensity relative to ^{195}Hg channel deduced from γ-ray yields (I_{SD}), energy ($E_{\gamma 0}$), and spin assignment ($I_i \rightarrow I_f$) of lowest transition, parity, signature exponent, and proposed quasineutron configuration.

Band	I_{SD} (%)	Lowest transition E_γ (keV)	Lowest transition $I_i \rightarrow I_f$ ($\hbar$)	Parity	Signature exponent (α)	Proposed configuration
(a)	0.4(2)	334	$\frac{33}{2} \rightarrow \frac{29}{2}$	+	$+\frac{1}{2}$	$[624]\frac{9}{2}$
(b)	0.9(3)	274	$\frac{27}{2} \rightarrow \frac{23}{2}$	+	$-\frac{1}{2}$	$[624]\frac{9}{2}$
(c)	0.4(1)	285	$\frac{29}{2} \rightarrow \frac{25}{2}$	−	$+\frac{1}{2}$	$j_{15/2}$
(d)	0.6(3)	342	$\frac{35}{2} \rightarrow \frac{31}{2}$	−	$-\frac{1}{2}$	$j_{15/2}$

tainly within the capabilities of the modern γ-ray arrays.

While a consistent picture seems to emerge, two difficulties with the interpretation presented above must be noted. First, the data do not show strong evidence for cross talk between bands (a) and (b); the intensity of possible band (a) peaks in coincidence with band (b) is $<10\%$, and for band (b) peaks in coincidence with band (a) the upper limit is 20%. In ^{193}Hg, this cross talk provided the best evidence for assigning the ν [624]9/2 configuration to two of the SD bands [22]. This issue may be resolved with a new measurement specifically directed towards ^{195}Hg that would not suffer from the strong background of ^{193,194}Hg transitions inherent in the present experiment. Second, band (b) is much more intense than band (a). Normally one would expect that the intensity of signature partners should be more similar. One possible explanation is that the observed spectrum arises from two or more nearly isospectral bands. If this were the case, one would expect to observe a measurable broadening of the gamma-ray peaks relative to the widths measured in other SD bands seen in this experiment. This approach was used successfully to disentangle two nearly degenerate SD bands in ^{193}Hg [22]. However, the peak widths for band (b) were found to be, within statistics, consistent with those measured for the ^{194}Hg SD bands. Thus, the reason for the intensity difference remains unclear.

V. SUMMARY

Four new γ-ray cascades have been assigned as SD bands in ^{195}Hg; they are summarized in Table II. The SD intensities are $\leqslant 1\%$ of the total population of this nucleus. Two of these bands exhibit no signature splitting, and a [624]9/2 quasineutron configuration is proposed, while the third and fourth behave like the two signatures of a $\nu j_{15/2}$ intruder configuration. These new bands do not exhibit any ''identical bands'' relationship with any other SD bands known in this mass region. This may suggest a change in the Hg SD core with increasing neutron number and, possibly, the presence of a new shell gap at $N=116$ which results in a new core with characteristics somewhat different from that at $N=112$.

ACKNOWLEDGMENTS

We thank the staff of the 88- Inch cyclotron facility at the Lawrence Berkeley National Laboratory for providing the beam. This work is supported by the U.S. Department of Energy under Contracts Nos. W-31-109-ENG-38 and DE-AC03-76SF00098. G.H. acknowledges support from the Natural Science and Engineering Research Council (Canada).

[1] R. R. Chasman, Phys. Lett. B **219**, 227 (1989).
[2] W. Satuła, S. Ćwiok, W. Nazarewicz, R. Wyss, and A. Johnson, Nucl. Phys. **A529**, 289 (1991).
[3] S. J. Krieger, P. Bonche, M. S. Weiss, J. Meyer, H. Flocard, and P.-H. Heenen, Nucl. Phys. **A542**, 43 (1992).
[4] E. F. Moore, R. V. F. Janssens, R. R. Chasman, I. Ahmad, T. L. Khoo, F. L. H. Wolfs, D. Ye, K. B. Beard, U. Garg, M. W. Drigert, Ph. Benet, Z. W. Grabowski, and J. A. Cizewski, Phys. Rev. Lett. **63**, 360 (1987).
[5] For a complete bibliography see B. Singh, R. B. Firestone, and S. Y. F. Chu, ''Table of Superdeformed Nuclear Bands and Fission Isomers,'' Report No. LBL-38004, 1995.
[6] For a review see R. V. F. Janssens and T. L. Khoo, Annu. Rev. Nucl. Part. Sci. **41**, 321 (1991).
[7] R. Wyss and W. Satuła, Phys. Lett. B **351**, 393 (1995).
[8] H. J. Lipkin, Ann. Phys. (N.Y.) **9**, 272 (1960); Y. Nogami, Phys. Rev. **134**, B313 (1964).
[9] J. Terasaki, P.-H. Heenen, P. Bonche, J. Dobaczewski, and H. Flocard, Nucl. Phys. **A593**, 1995.
[10] M. Girod, J. P. Delaroche, J. F. Berger, and J. Libert, Phys. Lett. B **325**, 1 (1994); L. Egido *et al.* (unpublished).
[11] G. Zwartz, Ph.D. thesis, University of Toronto, 1995.
[12] B. Cederwall *et al.*, Phys. Rev. C **47**, R2443 (1993).
[13] R. Krücken *et al.*, Phys. Rev. C **54**, 2109 (1996).
[14] M. A. Deleplanque and R. M. Diamond, GAMMASPHERE proposal, Report No. LBL-PUB-5202, 1988; I. Y. Lee, Nucl. Phys. **A520**, 641c (1990).
[15] D. S. Haslip, G. Hackman, and J. C. Waddington, Nucl. Instrum. Methods Phys. Res. A **345**, 534 (1994).
[16] D. C. Radford, Nucl. Instrum. Methods Phys. Res. A **361**, 306 (1995).
[17] G. Hackman and J. C. Waddington, Nucl. Instrum. Methods Phys. Res. A **357**, 559 (1995).
[18] D. Mehta, Y. K. Agarwal, K. P. Blume, S. Heppner, H. Hubel, M. Murzel, K. Theine, W. Gast, G. Hebbinghaus, R. M. Lieder, and W. Urban, Z. Phys. A **339**, 317 (1991).
[19] R. Bengtsson and S. Frauendorf, Nucl. Phys. **A327**, 139 (1979).

[20] J. A. Becker *et al.*, Phys. Rev. C **46**, 889 (1992); J. E. Draper *et al.*, *ibid.* **42**, R1791 (1990).
[21] M. P. Carpenter *et al.*, Phys. Rev. C **51**, 2400 (1995).
[22] M. Joyce *et al.*, Phys. Rev. Lett. **71**, 2176 (1993).
[23] R. Wyss, A. Oros, I. Wiedenhöver, and P. v. Brentano (unpublished).
[24] W. Nazarewicz, R. Wyss, and A. Johnson, Nucl. Phys. **A503**, 285 (1989).
[25] B. Cederwall *et al.*, Phys. Rev. Lett. **72**, 3150 (1994).
[26] C. Baktash, B. Haas, and W. Nazarewicz, Annu. Rev. Nucl. Part. Sci. **45**, 485 (1995).
[27] F. S. Stephens, Nucl. Phys. **A520**, 91c (1990); F. S. Stephens *et al.*, Phys. Rev. Lett. **64**, 2623 (1990).
[28] R. Wyss, (unpublished).